1.2 - The Josephson effect

This lecture will be based on references [1], [2] [3].

0 Intro

Until now we have seen that supercurrents could be induced by applying magnetic fields, electric fields and by the flux quantization condition. We will explore in this lecture another mechanism to drive supercurrents that is entirely quantum mechanical: a phase gradient $\nabla\theta$ of the macroscopic wavefunction. This is a result of quantum tunneling when an obstacle separates two superconducting materials, a configuration known today as a Josephson junction, after Brian Josephson [4] who predicted its effect in 1962 as an undergraduate student at Cambridge University. He received the Nobel prize for this discovery in 1973 [5].

Quantum tunneling is an effect displayed by many quantum systems with observable consequences. The most notable one is radioactive decay from particles in the nuclei escaping the strong force potential. Another, less known example, is electron tunneling through a thin insulating barrier.

Ivar Giaever was investigating normal metal-insulator-superconductor tunneling experiments when he observed that no current would flow until a voltage with magnitude Δ/e would be supplied to the material, as each electron in a broken pair will have at least an energy of Δ/e. This is in precise agreement with the BCS theory, where electrons are bound in pairs of energy 2Δ. Therefore, below Δ/e the system would display an infinite resistance, as experimentally observed, seen in the Fig. 1 When the other material is also superconducting, in order for normal electrons to

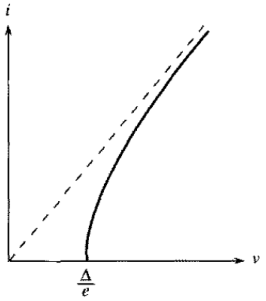

Figure 1: IV curve of a superconductor-insulator-normal junction. Source: Orlando.

overcome the energy gap of 2Δ, we need to supply a voltage of $2\Delta/e$ to the material. This is also observed in the experiment, as seen in Fig. 4. There is however another

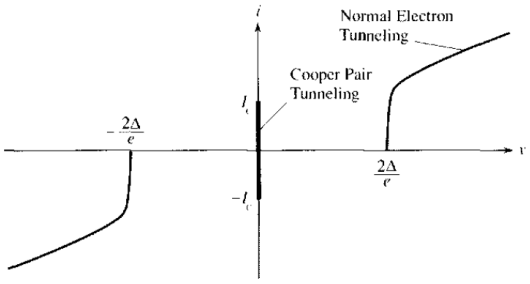

Figure 2: IV curve of a superconductor-insulator-superconductor junction. Source: Orlando.

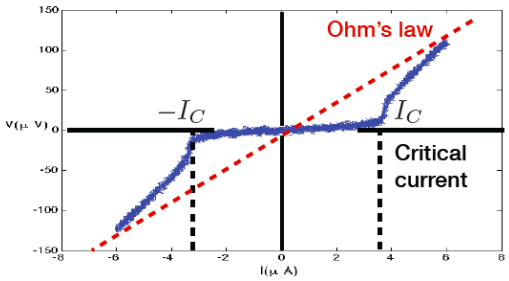

Figure 3: Experimental IV curve of a superconductor-insulator-superconductor junction [6]

possibility. What about Cooper pair tunneling? By 1962 it was believed not to be possible, as probability of an electron P_e tunneling would be small, a Cooper pair would go as $P_{CP} = (P_e)^2$, negligible. Brian Josephson changed that, showing that $P_e \sim P_{CP}$, due to the coherence in the BCS wavefunction. **The picture is not that of two electrons tunneling together, but of the macroscopic wavefunction tunneling from one superconductor to the next.** This was confirmed in 1963 by Anderson and Rowell [7].

IV of a Junction shows central supercurrent branch displaying no voltage drop, known as the Josephson current. It has a maximum value known as the critical current I_C. When the applied current exceeds the critical current, a voltage will be developed across the junction as single electron tunneling will start to take place. This has led to ideas to develop a digital logic with Josephson junctions.

When a DC voltage below the gap is applied, Cooper pairs oscillate back and forth. This results in the emission of em radiation, and therefore can be used as an oscillator. The opposite is also true, an oscillating voltage induces a DC voltage across the junction. This is the basis to define currently the voltage standard. Magnetic fields also affect the process of Cooper pair tunneling.

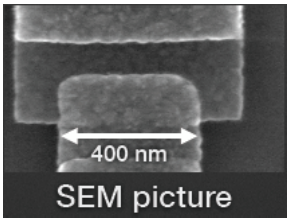

Figure 4: Scanning electron micrograph image of an aluminum-aluminum oxide-aluminum Josephson junction viewed from the top.

1 The Josephson equations

1.1 Josephson tunneling

Given a Josephson tunnel junction, from now on referred to simply as 'junction', we want to know what will the supercurrent J_s be in this configuration. In each superconducting lead, J_s will obey

$$\mathbf{J}_s = -\frac{1}{\Lambda}\left(\frac{\Phi_0}{2\pi}\nabla\theta(\mathbf{r},t) + \mathbf{A}(\mathbf{r},t)\right). \tag{1}$$

Here we used explicitly that we have Cooper pairs, so $q^* = -2e$, such that $\Lambda = m_{CP}/[n_{CP}(2e)^2]$, with m_{CP} and n_{CP} being the mass and density of Cooper pairs, respectively. The superconducting phase will follow the current-phase relation

$$\frac{\partial\theta(\mathbf{r},t)}{\partial t} = -\frac{1}{\hbar}\left[\frac{\Lambda\mathbf{J}_s^2}{2n_{CP}} - 2e\phi(\mathbf{r},t)\right]. \tag{2}$$

Approximations: small junction such that J_0 is uniform across area; vector potential $\mathbf{A} = 0$, so no external fields. Then, on each side of the junction,

$$\mathbf{J}_s(\pm a,t) = -\frac{\Phi_0}{2\pi\Lambda}\nabla\theta(\pm a,t) = J_0. \tag{3}$$

Here, the junction is assumed to have a thickness of $2a$ and lies on the yz plane. The phase equation in the absence of fields is

$$\frac{\partial\theta}{\partial t} = -\frac{1}{\hbar}\left(\frac{\Lambda\mathbf{J}_0^2}{2n_{CP}}\right) = -\frac{\mathcal{E}_0}{\hbar}, \tag{4}$$

where $\mathcal{E}_0$ is the kinetic energy of the superelectrons and it's a constant. The time dependent wave function becomes

$$\Psi(\pm a,t) = \Psi(\pm a)e^{-i\mathcal{E}_0 t/\hbar}, \tag{5}$$

with $\Psi(\pm a)$ the time-independent wave function. To find the wavefunction in the insulator $\Psi(\mathbf{r})$, we model the system as a constant potential barrier of height $V_0 > \mathcal{E}_0$. Classically, Cooper pairs would not be allowed to enter this region. Quantum mechanically we know this is not the case. Since the pairs must maintain the energy

$\mathcal{E}_0$, the problem can be reduced to solving the time independent Schrödinger equation in the forbidden region:

$$-\frac{\hbar}{2m^*}\nabla^2\Psi(x) = (\mathcal{E}_0 - V_0)\Psi(x), \text{ for } |x| < a. \tag{6}$$

The solution is made of combinations of real exponentials:

$$\Psi(x) = C_1 \cosh\frac{x}{\xi} + C_2 \sinh\frac{x}{\xi}, \tag{7}$$

with $\xi \equiv \hbar/\sqrt{2m^*(V_0 - \mathcal{E}_0)}$ is the decay length inside the insulator. We had obtained the expression for the supercurrent in the MQM model

$$\mathbf{J}_s = \frac{q^*}{m^*}\mathrm{Re}\left\{\Psi^*\frac{\hbar}{i}\nabla\Psi\right\}. \tag{8}$$

For the type of solution encountered in this case, the supercurrent becomes

$$\mathbf{J}_s = \frac{q^*\hbar}{m^*\xi}\mathrm{Im}(C_1^* C_2). \tag{9}$$

Note that it is independent of x, as expected from current continuity. To find the coefficients C_1 and C_2 we define the value of the wavefunction at each end of the junction as our boundary conditions:

$$\Psi(-a) = \sqrt{n_1^*}e^{i\theta_1}, \tag{10}$$

$$\Psi(+a) = \sqrt{n_2^*}e^{i\theta_2}. \tag{11}$$

The solution (left as an exercise) is

$$\boxed{\mathbf{J}_s = J_c \sin(\theta_1 - \theta_2),} \tag{12}$$

where

$$J_c \equiv \frac{q^*\hbar}{2m^*\xi}\frac{\sqrt{n_1^* n_2^*}}{\sinh(a/\xi)\cosh(a/\xi)} = \frac{e\hbar}{2m\xi}\frac{\sqrt{n_1 n_2}}{\sinh(2a/\xi)}, \tag{13}$$

is known as the junction critical current density. Here we changed the constants for those a Cooper pair, $q^* = 2e$, $m^* = 2m_e$, $n^* = n/2$. In usual experiments $a/\xi \ll 1$, so $\sinh(2a/\xi) \approx e^{2a/\xi}/2$, showing an exponential dependence of the critical current density on the junction thickness.

Equation. (12) is known as the Josephson current-phase relation or first Josephson equation. This relation states that Cooper pairs tunnel through a barrier separating two superconductors. As we had initially stated in this lecture, a phase gradient does drive a supercurrent. The surprise was to find that this supercurrent depends sinusoidally on the phase difference across the junction.

In a more general three-dimensional junction, this relation can be generalized to assume that the critical current density depends on the transverse coordinates $\mathbf{J}_c(y, z)$ for a junction axis along the x direction.

In the presence of a magnetic field, we need to replace the phase difference $\theta_1 - \theta_2$ by its gauge-invariant version. As we saw in the previous lecture, the phase between two gauges is related by

$$\theta' = \theta - \frac{2\pi}{\Phi_0}\chi, \tag{14}$$

which leads to

$$\theta_1' - \theta_2' = \theta_1 - \theta_2 - \frac{2\pi}{\Phi_0}(\chi_1 - \chi_2). \tag{15}$$

By defining the gauge-invariant phase $\varphi \equiv \theta_1' - \theta_2'$, we can write the most general version of the current-phase relation as

$$\boxed{\mathbf{J}_s(\mathbf{r}, t) = \mathbf{J}_c(y, z, t) \sin \varphi(y, z, t),} \tag{16}$$

with

$$\boxed{\varphi(y, z, t) = \theta_1(y, z, t) - \theta_2(y, z, t) - \frac{2\pi}{\Phi_0}\int_1^2 \mathbf{A}(\mathbf{r}, t) \cdot d\mathbf{l}.} \tag{17}$$

where we have connected the function χ with the vector potential as

$$\chi_1 - \chi_2 = \int_1^2 \mathbf{A}(\mathbf{r}, t) \cdot d\mathbf{l}, \tag{18}$$

where the line integral is taken across the insulator in the direction of the current, from θ_1 to θ_2. It can be shown that these relations also hold for an externally applied magnetic field.

Now let's look at the dynamics of the gauge-invariant phase difference. Taking the time derivative of Eq. (17),

$$\frac{\partial \varphi}{\partial t} = \frac{\partial \theta_1}{\partial t} - \frac{\partial \theta_2}{\partial t} - \frac{2\pi}{\Phi_0}\frac{\partial}{\partial t}\int_1^2 \mathbf{A}(\mathbf{r}, t) \cdot d\mathbf{l}. \tag{19}$$

Using the energy-phase relation, Eq (2) and current conservation $\mathbf{J}_s(a) = \mathbf{J}_s(-a)$,

$$\frac{\partial \varphi}{\partial t} = \frac{2\pi}{\Phi_0}\int_1^2 \left(-\nabla\phi - \frac{\partial \mathbf{A}}{\partial t}\right) \cdot d\mathbf{l} \tag{20}$$

The term in parenthesis is just the electric field, $\mathbf{E} = -\nabla\phi - \partial\mathbf{A}/\partial t$. The line integral of the electric field is the voltage across the junction. Therefore, we write

$$\boxed{\frac{\partial \varphi(y, z, t)}{\partial t} = \frac{2\pi}{\Phi_0} V(y, z, t).} \tag{21}$$

This equation is known as the Josephson voltage-phase relation, or also the Second Josephson equation.

1.1.1 Microscopic theory of Josephson junctions

Equation (13) is the result of our simplified MQM. The exact result using the microscopic BCS theory was developed originally by Josephson and later complemented by the reference work of Ambegaokar and Baratoff, including the full temperature dependence of I_c, leading to [8]

$$I_c R_n = \frac{\pi\Delta}{2e} \tanh\left(\frac{\Delta}{k_B T}\right), \tag{22}$$

where R_n is the value of the junction resistance in its normal state. This expression is widely used in experiments involving Josephson junctions as it allows one to predict properties of the superconducting state (the critical current I_c) with properties obtained from measurements in the normal metal state, such as the resistance R_n.

1.2 Lumped junctions

In the usual electrical circuits we will be considering when discussing superconducting qubits, the gauge-invariant phase relation and the current density will be uniform across the junction. Such a junction will be termed basic lumped junction. In this case, we can defined a current $i = \int \mathbf{J} \cdot d\mathbf{s}$ and critical current $I_C = \int \mathbf{J}_c \cdot d\mathbf{s}$. Then, the Josephson relations reduce to

$$\boxed{\begin{aligned} i &= I_C \sin\varphi(t), && (23)\\ \frac{d\varphi}{dt} &= \frac{2\pi}{\Phi_0} V, && (24)\\ \varphi(t) &= \theta_1(t) - \theta_2(t) - \frac{2\pi}{\Phi_0}\int_1^2 \mathbf{A}(\mathbf{r},t)\cdot d\mathbf{l}. && (25) \end{aligned}}$$

In order to calculate the energy stored in the junction, consider the work done by an external current source to change the current through the junction from zero to a finite value. In this process the phase will be changing in time, leading to the generation of a voltage. Therefore, a power iV will be spent by the source in the process. The energy U_J stored in the junction is

$$U_J = \int_0^t iV dt' = \int_0^t (I_C \sin\varphi)\left(\frac{\Phi_0}{2\pi}\frac{d\varphi}{dt'}\right) dt' \tag{26}$$

Changing variables of integration from t' to φ', yields

$$\boxed{U_J = \frac{\Phi_0 I_C}{2\pi}(1-\cos\varphi) \equiv E_J(1-\cos\varphi).} \tag{27}$$

This is the Josephson potential energy of a junction, with $E_J = I_C\Phi_0/2\pi$ being known as the Josephson energy of a junction.

When a time dependent voltage drives the junction complex dynamics start to take place. Let's assume the voltage to be constant in time V_0. The phase φ will change linearly as

$$\varphi(t) = \varphi(0) + \frac{2\pi}{\Phi_0} V_0 t, \tag{28}$$

leading to an oscillating supercurrent

$$i(t) = I_C \sin(\varphi(0) + 2\pi f_J t), \tag{29}$$

where we defined the Josephson frequency $f_J = V_0/\Phi_0 = 483.6 \times 10^{12} V_0$ (Hz). This effect is known as the ac Josephson effect [1] and is the basis for the definition of the voltage standard, since its value is given by fundamental constants. A constant drive of 10 μV will lead to a frequency of 5 GHz, bringing the system response in the microwave regime. The junction may emit such type of radiation, therefore acting as an oscillator. The reverse is also true, external radiation will induce a constant DC voltage across the junction.

A final, and most important, remark regarding Josephson junctions is their constitutive current-voltage relation. Let us take the time derivative of current,

$$\frac{di}{dt} = I_C \cos(\varphi(t)) \frac{d\varphi}{dt} = V \left[\frac{2\pi}{\Phi_0} \sqrt{I_C^2 - i^2} \right]. \tag{30}$$

Here, we used $\cos\varphi = \sqrt{1 - \sin^2\varphi}$. Clearly, there is a nonlinear relationship between the time derivative of current and the voltage across the junction. Going back to classical electrical circuits, we realize that the term between brackets corresponds to the inverse of an inductance. We then define the Josephson inductance of a junction:

$$\boxed{L_J \equiv \frac{\Phi_0}{2\pi I_C \sqrt{1 - \left(\frac{i}{I_C}\right)^2}} = \frac{\Phi_0}{2\pi I_C \cos\varphi.}} \tag{31}$$

For small currents across the junction $i/I_C \ll 1$,

$$L_J \simeq \frac{\Phi_0}{2\pi I_C}. \tag{32}$$

We see then that the junction in the small current limit behaves like a linear, constant inductance. Using typical values of $I_C = 100$ nA, this yields an inductance of $L_J = 3.3$ nH, which is a very large quantity given the small footprint of the junction, typically well below 1 μm^2.

1.3 The RCSJ model

So far, we considered Josephson junctions to be circuit components with just a tunneling supercurrent. In real life, Josephson tunnel junctions, the ones used in superconducting qubits, have a parallel-plate-like geometry and therefore have capacitance. In addition, for currents exceeding the critical current I_c normal electron tunneling occurs. Besides, at finite temperatures below T_C, unpaired electrons may also tunnel through, therefore requiring a resistive channel to model these effects. Altogether, leads to the so-called RCSJ model of Josephson junctions which is widely used in their characterization experimentally.

The RCSJ model desribes a Josephson junction by an ideal one given by Eq. (23) shunted by a resistance R and a capacitance C, as sketched in the figure below. R

accounts for the dissipation in the finite voltage regime, without affecting the lossless dc regime. It also does not account for leaky currents found in lossy dielectrics. C reflects the geometric shunting capacitance between the two junction electrodes, not the capacitances to ground. Near T_c, $R \sim R_n$, the normal state resistance of the

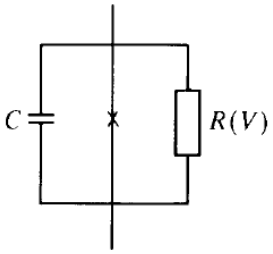

Figure 5: RCSJ model of a Josephson tunnel junction. Source: Tinkham.

junction leads. At lower temperatures, $R \sim R_n e^{\Delta/k_B T}$ for $V < V_g \equiv 2\Delta/e$. This expression takes into account the freezing effect of quasiparticles as temperature is lowered below T_c. Ideally, one may model a linear, voltage-dependence resistance shunting the junction with values

$$R(V) = \begin{cases} R_{sg}(T) & \text{if } |V| < 2\Delta/e, \\ R_n & \text{if } |V| > 2\Delta/e. \end{cases}$$

Besides this linear resistance, Josephson already remarked in his original work the existence of another phase-dependent dissipative term reflecting an interference between the pair and quasi-particle currents, giving rise to a current $VG_{\text{int}} \cos\varphi$, G_{int} being the conductance of such a channel. Experiments prior to the qubit era could not agree on the sign of this conductance, but suggested $G_{\text{int}} \sim \pm 1/R(V)$. It was using one type of flux-like qubit known as the fluxonium qubit (to be studied in Chapter 2 of this course) that it was verified this term was exactly -1 by observing the enhancement of qubit lifetime when biased at exactly $\Phi_0/2$ where this term vanishes [9].

In the presence of an externally applied current bias I, the time dependence of the phase φ across the junction can be obtained by current conservation

$$I = I_C \sin\varphi + \frac{V}{R} + C\frac{dV}{dt}. \tag{33}$$

Introducing the second Josephson equation,

$$\frac{I}{I_C} = \sin\varphi + (\omega_p Q)^{-1}\dot{\varphi} + \omega_p^2 \ddot{\varphi}. \tag{34}$$

We defined in this last equation the plasma frequency of the Josephson junction

$$\boxed{\omega_p \equiv \sqrt{\frac{2\pi}{\Phi_0}\frac{I_c}{C}},} \tag{35}$$

and the junction quality factor

$$Q \equiv \omega_p RC, \tag{36}$$

in analogy to RLC resonators. ω_p will be very important for the transmon qubits presented in chapter 2.

Thus, the junction dynamics is described (not suprisingly) by a complex nonlinear differential equation. In order to elucidate its dynamics, consider the tilted washboard potential, which is in fact describing the junction dynamics

$$U(\varphi) = -E_J \cos\varphi - \frac{\Phi_0 I}{2\pi}\varphi, \tag{37}$$

subjected to a viscous force $(\Phi_0/2\pi)^2(1/R)\dot{\varphi}$. The geometric significance of I_C is that when $I = I_c$, the local minima of the tilted cosine become horizontal inflection points in a downward slope, so that for $i \geq I_c$ no stable equilibrium point exists. Figure 6 shows a progressively larger bias in a junction. Intuitively, we have a

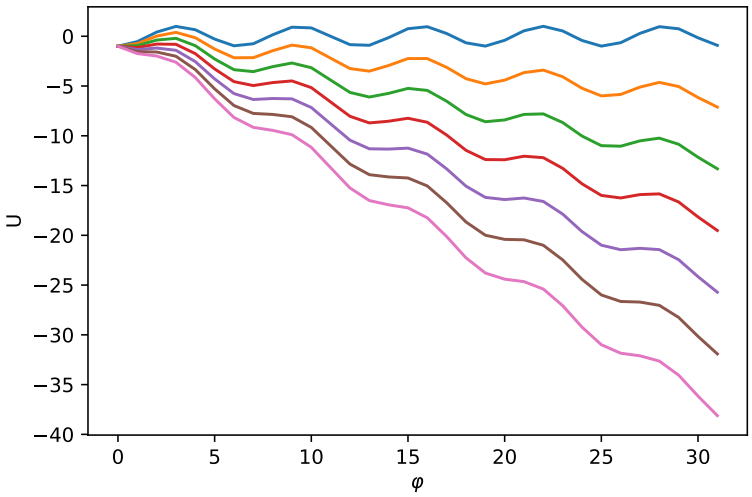

Figure 6: Tilted washboard potential of a current biased junction.

particle moving in a gravitational field along a track with potential $U(\varphi)$. Both thermal and quantum fluctuations may lead to the particle to escape the potential for sufficient tilt. This was relevant for a primitive type of superconducting qubit known as the phase qubit, originally investigated as far back as 1985, well before the advent of superconducting qubits [10].

The value of Q determines the type of junction. For $Q > 1$ one has underdamped junctions, which exhibit practically no dissipation below the critical current. On the contrary, overdamped junctions have $Q < 1$ and active dissipation through the resistive channel takes place at all bias currents. These type of junctions aren't suitable for qubits due to the noise they generate, but are widely used in sensing of magnetic fields and vibrations [11] and in digital superconducting logic known as Rapid Flux Quantum (RFSQ) [12].

2 Applications of the Josephson effect: SQUIDs

Having obtained the equations of motion for Josephson junctions, we can now start defining novel type of electrical circuits based on this components. We will discuss in this section a device known as the DC superconducting quantum interference device (DC-SQUID), which will become extremely ubiquitous in the designing of superconducting qubits. A different type of magnetometer also used in qubit circuits is known as the rf-SQUID consisting of a single junction in a superconducting loop. We will not describe it here but it will be part of one of the assignments of this course.

Take two junctions combined in parallel, as shown in Fig. (7). For simplicity let's take both junctions to be identical. Then, the total i_{SQ} current will be given by

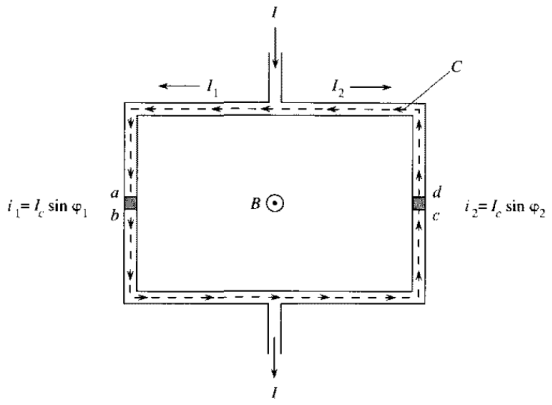

Figure 7: Two junctions in parallel form a DC-SQUID. Source: Orlando

$$i_{SQ} = i_1 + i_2 = I_C \sin\varphi_1 + I_C \sin\varphi_2 \tag{38}$$

$$= 2I_C \cos\left(\frac{\varphi_1 - \varphi_2}{2}\right) \sin\left(\frac{\varphi_1 + \varphi_2}{2}\right). \tag{39}$$

The gauge invariant phase difference can be obtained by integrating the phase $\nabla\theta$ around the closed path C shown in the figure. We have

$$\oint_C \nabla\theta \cdot d\mathbf{l} = (\theta_b - \theta_a) + (\theta_c - \theta_b) + (\theta_d - \theta_c) + (\theta_a - \theta_d) = 2\pi n. \tag{40}$$

The last equality considers the multivaluedness of θ upon completing the path of integration in the closed loop C. From the last equation, the first and third terms correspond to the phase drop across each junction and their value is obtained from the gauge invariance phase definition

$$\theta_b - \theta_a = -\varphi_1 - \frac{2\pi}{\Phi_0}\int_a^b \mathbf{A} \cdot d\mathbf{l}, \tag{41}$$

$$\theta_d - \theta_c = +\varphi_2 - \frac{2\pi}{\Phi_0}\int_c^d \mathbf{A} \cdot d\mathbf{l}. \tag{42}$$

Note the sign convention for φ_1 and φ_2 in defining the phase difference along the contour C. The second and fourth terms correspond to the phase differences along the superconducting wire. These are obtained from the supercurrent equation, Eq. (1)

$$\theta_c - \theta_b = -\frac{2\pi}{\Phi_0}\left[\int_b^c \Lambda \mathbf{J}\cdot d\mathbf{l} + \int_b^c \mathbf{A}\cdot d\mathbf{l}\right] \tag{43}$$

$$\theta_a - \theta_d = -\frac{2\pi}{\Phi_0}\left[\int_d^a \Lambda \mathbf{J}\cdot d\mathbf{l} + \int_d^a \mathbf{A}\cdot d\mathbf{l}\right]. \tag{44}$$

Together, this leads to

$$\varphi_2 - \varphi_1 = 2\pi n + 2\pi\frac{\Phi}{\Phi_0} + \frac{2\pi}{\Phi_0}\int_{C'} \Lambda \mathbf{J}\cdot d\mathbf{l}, \tag{45}$$

where we used that the line integral of the vector potential around the loop corresponds to the magnetic flux Φ, and we also defined the path C' as that not containing the junctions. This equation is also known as the phase quantization condition and it is analogous to flux quantization.

For simplicity let's assume first that we are using a thick superconducting wire and take C' to lie well within the penetration depth where current is null $\mathbf{J} = 0$. Then, the total current will be given by

$$i_{SQ} = 2I_C\cos(\pi f)\sin(\varphi_1 + \pi f) = I_{SQ}(\Phi)\sin(\varphi_1 + \pi f), \tag{46}$$

where $f \equiv \Phi/\Phi_0$ is defined as the frustration. The total flux is the sum of the externally applied flux and the flux generated by the currents in the loop. We define the average current $\bar{I} \equiv (i_1 + i_2)/2$ and the circulating current $I_{\rm circ} \equiv (i_1 - i_2)/2$, which generates flux $LI_{\rm circ}$. The total flux is then

$$\Phi = \Phi_{\rm ext} + LI_{\rm circ} = \Phi_{\rm ext} + \frac{LI_C}{2}(\sin\varphi_1 - \sin\varphi_2). \tag{47}$$

Using Eq. (45),

$$\Phi = \Phi_{\rm ext} - LI_c\sin(\pi f)\cos(\varphi_1 + \pi f). \tag{48}$$

This equation and Eq. (46) have to be solved self-consistently to describe the SQUID response, which will strongly depend on the value of LI_C. Experimentally the quantity often most relevant to determine from the SQUID is the maximum current $i_{\rm Max}$ before a voltage appears across the SQUID.

- $LI_C \ll \Phi_{\rm ext}$. Then, $\Phi \simeq \Phi_{\rm ext}$. The maximum current $i_{\rm Max} \equiv \partial i_{SQ}/\partial\varphi_1 = 0$, leading to

  $$i_{\rm Max} = 2I_C|\cos(\pi f)|. \tag{49}$$

  This results in a periodic modulation of the critical current with flux. We see now that Eq. (46) looks very much like the supercurrent of an individual Josephson junction with an effective critical current $I_C(\Phi) \equiv 2I_C\cos(\pi f)$ that can be tuned with the external flux threading the loop $\Phi_{\rm ext}$, showing a periodicity with the flux quantum Φ_0. This is precisely the basis of the DC-SQUID as a magnetometer. A 2 cm^2 DC-SQUID shows a periodic modulation

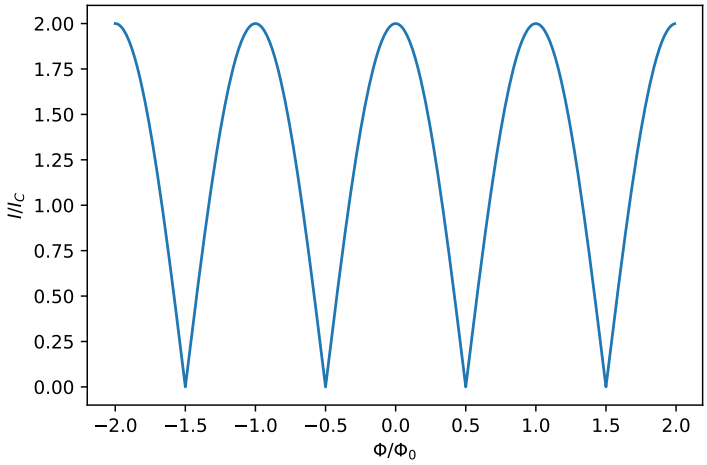

Figure 8: SQUID critical current modulation with external flux.

every 10 pT, well enough to detect magnetic fields from the human brain (∼fT) [1]. Note that in this case, the loop inductance L_G is so small that it cannot screen the external flux, so no flux quantization is observed.

- $LI_C \simeq \Phi_{\text{ext}}$. In this general case, there are no easy approximations and Eqs. (46, 48) have to be numerically evaluated. Figure 9 shows the critical current modulation for a SQUID with $L/L_J = 0.33$, leading to a reduction in the lower critical current obtained in the region near half integer flux quanta, $N\Phi_0/2$. For loops with larger inductance, the total flux starts to develop a step-like pattern, as seen in Fig. 10. This is because the SQUID will look more and more like a single loop, where the flux will be quantized as $\Phi = \Phi_{\text{ext}} + LI_{\text{circ}} \approx n\Phi_0$, where n is the nearest integer to Φ/Φ_0. Differently from a closed loop, a loop with a junction will have φ to assume any value, and it will thus always maintain the lowest energy state (corresponding to the lowest circulating current) by adjusting the value of fluxoids n.

Let us now consider the more general case that the SQUID is not formed out of thick superconducting leads (as is the case of qubits), so the superconducting current is not negligible, in other words the kinetic inductance L_k is not small. Let us also include the geometric inductance of the loop L_g that generates a screening magnetic flux whenever an external flux is applied. Going back to the phase quantization condition Eq. (45) we can rewrite it as

$$\varphi_2 - \varphi_1 = 2\pi n + 2\pi \frac{\Phi_{\text{ext}}}{\Phi_0} + \frac{2\pi}{\Phi_0}(L_k + L_g)I_{\text{circ}}, \tag{50}$$

where we joined geometric inductance L_g, being the flux-generating one, and also the one carrying the kinetic part of the superconducting phase drop modelled with the kinetic inductance L_k, as explained in the previous lecture. We see here the

[1] Such developments are indeed taking place, see for example [13]

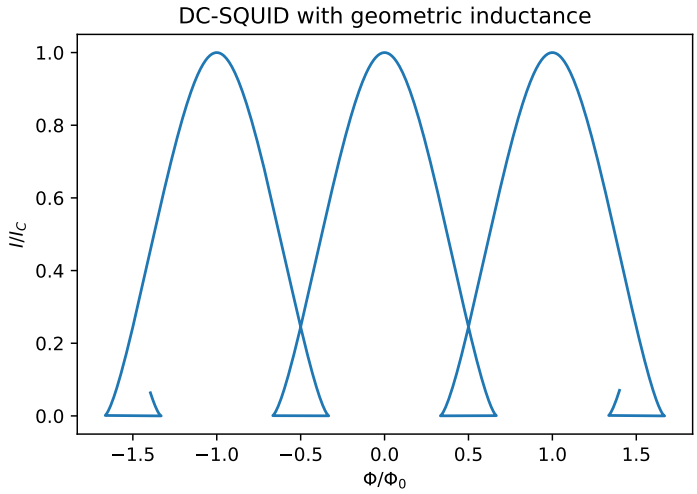

Figure 9: SQUID critical current modulation with external flux with geometric inductance in the loop with $\beta = 0.33$. In the region with 2 solutions, only the one with higher critical current is valid, thus reducing the swing of I_C from the lower side as compared to the case with no geometric inductance.

parallel role played by both the kinetic L_k and geometric L_g inductances. Together, the total current in the SQUID, Eq. (38), and the phase quantization condition, we obtain the two constitutive equations for the SQUID

$$\varphi_2 - \varphi_1 = 2\pi n + 2\pi \frac{\Phi_{\text{ext}}}{\Phi_0} + \frac{2\pi}{\Phi_0}(L_k + L_g) \sin\left(\frac{\varphi_2 - \varphi_1}{2}\right) \cos\left(\frac{\varphi_2 + \varphi_1}{2}\right). \tag{51}$$

$$I_b = 2I_C \cos\left(\frac{\varphi_2 - \varphi_1}{2}\right) \sin\left(\frac{\varphi_2 + \varphi_1}{2}\right). \tag{52}$$

I_b represents the externally applied bias current to the SQUID, assuming it is always below the critical current. This equation can be solved self-consistently to obtain a relation between external $\varphi_1 + \varphi_2$ and internal $\varphi_1 - \varphi_2$ phases as function of the external variables (I_b, Φ_{ext}). This yields the SQUID critical current response as function I_b, Φ_{ext}. The resulting effect of the self-inductances of the SQUID (L_g, L_k) is to reduce the modulation depth of the critical current as function of the external flux, as seen in Fig. 9.

References

[1] Orlando, T. P. & Delin, K. A. *Foundations of Applied Superconductivity* (Prentice Hall, 1991), 1st edn.

[2] Feynman, Lighton & Sands. *The Feynman Lectures on Physics, volume III* (Addison-Wesley Publishing Company, 1963). URL `https://www.feynmanlectures.caltech.edu/`.

[3] Tinkham, M. *Introduction to superconductivity* (Dover Publications, 1996).

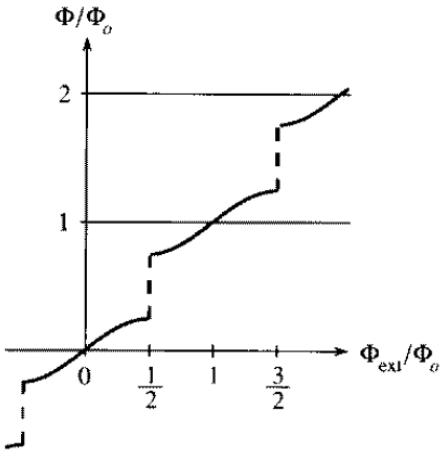

Figure 10: Total flux in a SQUID with a large geometric inductance.

[4] Josephson, B. Possible new effects in superconductive tunnelling. *Physics Letters* **1**, 251–253 (1962). URL https://www.sciencedirect.com/science/article/pii/0031916362913690.

[5] Josephson, B. D. The discovery of tunnelling supercurrents. *Rev. Mod. Phys.* **46**, 251–254 (1974). URL https://link.aps.org/doi/10.1103/RevModPhys.46.251.

[6] Forn-Díaz, P., Schouten, R. N., den Braver, W. A., Mooij, J. E. & Harmans, C. J. P. M. Josephson squelch filter for quantum nanocircuits. *App. Phys. Lett.* **95**, 042505 (2009). URL http://dx.doi.org/10.1063/1.3186047.

[7] Anderson, P. W. & Rowell, J. M. Probable observation of the josephson superconducting tunneling effect. *Phys. Rev. Lett.* **10**, 230–232 (1963). URL https://link.aps.org/doi/10.1103/PhysRevLett.10.230.

[8] Ambegaokar, V. & Baratoff, A. Tunneling between superconductors. *Phys. Rev. Lett.* **10**, 486–489 (1963). URL https://link.aps.org/doi/10.1103/PhysRevLett.10.486.

[9] Pop, I. M. *et al.* Coherent suppression of electromagnetic dissipation due to superconducting quasiparticles. *Nature* **508**, 369–372 (2014). URL https://doi.org/10.1038/nature13017.

[10] Martinis, J. M., Devoret, M. H. & Clarke, J. Energy-level quantization in the zero-voltage state of a current-biased josephson junction. *Phys. Rev. Lett.* **55**, 1543–1546 (1985). URL https://link.aps.org/doi/10.1103/PhysRevLett.55.1543.

[11] Etaki, S. *et al.* Motion detection of a micromechanical resonator embedded in a d.c. squid. *Nature Physics* **4**, 785–788 (2008). URL https://doi.org/10.1038/nphys1057.

[12] Bunyk, P., Likharev, K. & Zinoviev, D. *International Journal of High Speed Electronics and Systems* **11**, 257 (2001).

[13] Körber, R. *et al.* Squids in biomagnetism: a roadmap towards improved healthcare. *Superconductor Science and Technology* **29**, 113001 (2016).